A tri-functional vanadium(IV) complex to detect cysteine oxidation

Agostino Cilibrizzi,[a,b,c] Marina Fedorova,[a,b] Juliet Collins,[a,b] Robin Leatherbarrow,[a,d] Rudiger Woscholski,[a,b] Ramon Vilar*[a,b]

[a]*Department of Chemistry, Imperial College London, London SW7 2AZ, UK*

[b]*Institute of Chemical Biology, Imperial College London, London SW7 2AZ, UK*

[c]*Current address: Institute of Pharmaceutical Science, King's College London, London SE1 9NH, UK*

[d]*Current address: Liverpool John Moores University, Egerton Court, Liverpool L1 2UA, UK*

Correspoding author: r.vilar@imperial.ac.uk

ABSTRACT

The development of effective molecular probes to detect and image the levels of oxidative stress in cells remains a challenge. Herein we report the design, synthesis and preliminary biological evaluation of a novel optical probe to monitor oxidation of thiol groups in cysteine-based phosphatases (CBPs). Following orthogonal protecting approaches we synthesised a new vanadyl complex designed to bind to CBPs. This complex is functionalised with a well-known dimedone derivative (to covalently trap sulfenic acids, SOHs) and a coumarin-based fluorophore for optical visualization. We show that this new probe efficiently binds to a range of phosphatases *in vitro* with nanomolar affinity. Moreover, preliminary flow cytometry and microscopy studies in live HCT116 cells show that this probe can successfully image cellular levels of sulfenic acids – one of the species resulting from protein oxidative damage.

INTRODUCTION

A large number of proteins and enzymes are chemoselectively targeted by reactive oxygen species (ROS) via oxidation of cysteine residues.[1,2] Several studies have proposed oxidation as an important mechanism to regulate and control, as well as alter, essential cellular functions.[2-4] The heterogeneous family of cysteine-based phosphatases (CBPs), also referred to as 'protein tyrosine phosphatases' (PTPs), is known to undergo oxidative modifications that lead to changes in their activity which in turn have an impact on cell growth and homeostasis.[5,6] It has been demonstrated that the catalytic cysteine of CBPs (which has a low pKa) can be easily turned into a cysteine thiolate and subsequently oxidized by reaction with ROS (mainly H_2O_2) leading to the inhibition of its phosphatase activity.[7] Among the different forms of thiol oxidation, transient and reversible sulfenic acids (SOHs) are the first products to form in ROS-mediated oxidation of a generic cysteine. This process has been proposed to preserve enzymes from further reaction due to excessive ROS stimuli.[8,9] Recent studies,

have shown that the dynamic nature of SOH modifications (i.e. reversibility, allowing thiol regeneration) is a way to regulate CBP activity. Furthermore, this is a marker of initial protein oxidative damage, which has been associated to pathologies such as cancer, diabetes and neurodegenerative disorders.[1,10] Consequently, sulfenylation is considered a prominent post-translational modification (PTM),[5,8,11] leading to a variety of biochemical transformations and additional protein thiol oxidation forms (e.g. disulfide bond, S-glutathiolation and, cyclic sulfonamide, as well as largely irreversible sulfinic and sulfonic acids).

Chemical probes for SOH detection represent promising means to elucidate signalling pathways and regulatory mechanisms involving cysteine oxidation and redox regulation in CBPs. Therefore, extensive work has gone into developing targeted tools to identify sulfenic residues.[12-15] By exploiting the unique chemical reactivity of this sulfur species, several small-molecules have been recently developed which react with SOH cysteines both *in vitro* and in cells. A family of molecules which has been widely used for this purpose are derivatives of 5,5-dimethyl-1,3-cyclohexanedione, also known as dimedones (see 'SOH targeting group' in Figure 1c).[12-19]

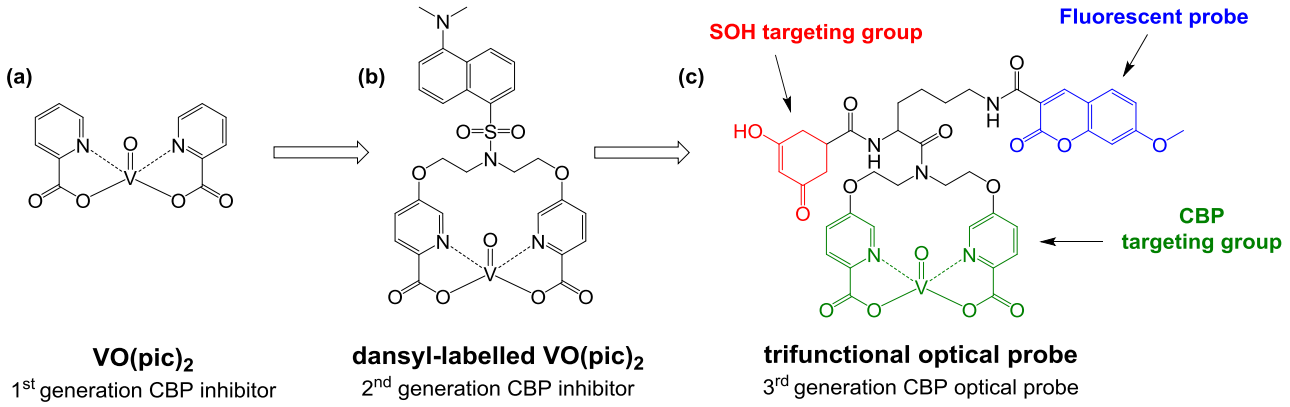

Figure 1. Rational design of trifunctional optical probe. (a) Chemical structure of the previously validated CBP inhibitor [$VO(pic)_2$];[23-25] (b) Chemical structure of a previously reported optical probe based on coupling dansyl fluorophore with a $VO(pic)_2$ core;[26] (c) Chemical structure of the trifunctional probe reported in this study containing a CPB-targeting moiety (i.e. $VO(pic)_2$), a coumarine-based fluorophore for imaging and a dimedone derivative to target SOH.

However, selective and potent tools to monitor sulfenic modifications on a specific family of enzymes are still largely unavailable and improvements to the existing methods for generic SOH identification are required.[20] Carroll's group recently reported the only example of an optical probe able to selectively detect oxidative modifications of PTPs (in particular YopH and PTP1B) with micromolar affinity.[21] While this probe has provided interesting insights into the oxidative processes of PTPs, it relies on an indirect visualization method via streptavidin/biotin visualization.[21,22]

Previously, vanadyl complexes such as [$VO(pic)_2$] (Figure 1(a)) have been shown to be very good inhibitors for phosphatases,[23-25] and consequently, $VO(pic)_2$ represents a good candidate to use as targeting motif for the enzymes of interest. More recently, we have successfully modified the dipicolinic vanadyl *core* through introduction of a bridge between the two picolinic residues.[26] This allowed us to further functionalize the vanadyl complex and introduce a dansyl fluorophore for optical visualization (Figure 1(b)). Most importantly, the introduction of the fluorophore did not have a major impact on the activity of the [$VO(pic)_2$] towards CBPs (the functionalized complex retained the nanomolar affinity for CBPs).[26]

Herein we report the further chemical manipulation carried out on the [$VO(pic)_2$] scaffold through the design, synthesis and preliminary biological evaluation of a new optical probe, with the ultimate aim to selectively detect and directly visualize SOH oxidation on CBPs. In addition to the [$VO(pic)_2$] *core* for CBP targeting, the new vanadyl complex contains a dimedone derivative and a coumarine-based fluorophore (Figure 1(c)), for both SOH detection (under oxidative conditions) and optical visualization *in vitro* and *in cellulo*.

RESULTS AND DISCUSSION

Synthesis of the trifunctional optical probe

The syntheses of the target dimedone-coumarine ligand **14** and the corresponding vanadyl complex **16** are outlined in Schemes 1 and 2 respectively. Two synthetic routes were originally investigated to prepare the protected precursor **14** starting with the bridged di-picolinic compound **1**.[26] The full synthetic design is based on a tri-orthogonal strategy by using in parallel two lysine scaffolds (i.e. Nα-Boc-Nε-Fmoc-L-Lys and Nα-Fmoc-Nε-Boc-L-Lys) with swapped protections on the amino groups (Scheme 1). This approach allowed us to determine the most useful protecting group in each position and the correct de-protection order in the synthesis of the methyl-protected compound **14**.

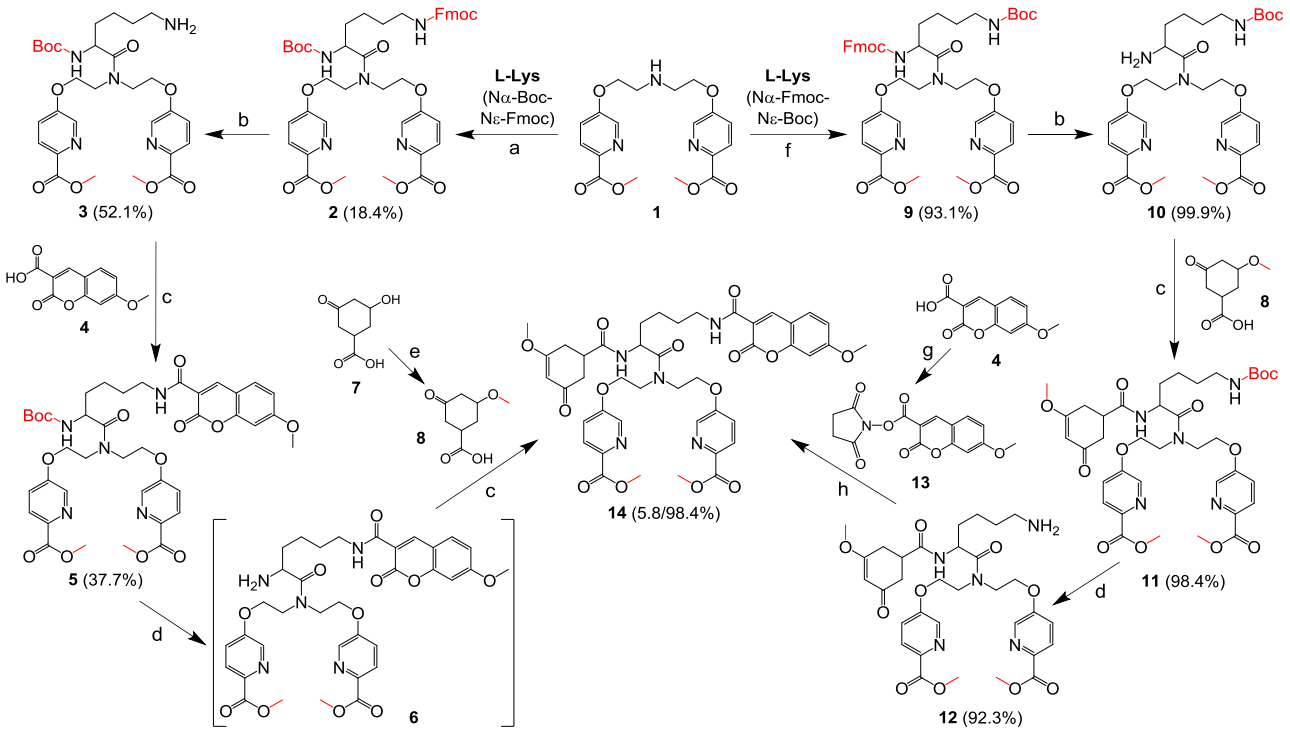

Scheme 1. Tri-orthogonal approach for the synthesis of fully protected precursor **14**. Reagents and conditions: **a)** *N*α-Boc-Nε-Fmoc-L-Lys (1.0 equiv), HATU (1.2 equiv), DIPEA (3.5 equiv), DMF, N_2, 7 h, rt; **b)** 60 °C; piperidine/CH_3CN 1:4, o/n, rt; **c)** HOBt (1.0 equiv), Et_3N (1.4 equiv), EDC (1.4 equiv), **4** or **8** (1.1-1.4 equiv), DMF, N_2, 48 h, rt; **d)** TFA/CH_2Cl_2 1:2, 2 h, rt; **e)** TsOH (0.05 equiv), CH_3OH, 1 h, rt; **f)** Nα-Fmoc-Nε-Boc Lys (1.0 equiv), TBTU (1.5 equiv), DIPEA (3 equiv), DMF, N_2, 6 h, rt; **g)** NHS (1.0 equiv), DCC (1.1 equiv), DMF, 5 h, 0 °C → rt; **h)** DMAP (0.1 equiv), DIPEA (2.0 equiv), **13** (0.95 equiv), CH_2Cl_2, N_2, 22 h, rt.

In the first route investigated, compound **1** was firstly reacted with Nα-Boc-Nε-Fmoc-L-Lys to yield compound **2**, using HATU (2-(7-aza-1*H*-benzotriazol-1-yl)-*N,N,N',N'*-tetramethylaminium hexafluorophosphate) as coupling reagent. After standard piperidine-mediated Fmoc removal, compound **3** was converted into **5** *via* amide coupling with 7-methoxycoumarin-3-carboxylic acid (**4**), in the presence of EDC, HOBt and Et_3N. Standard Boc removal using TFA afforded **6** which was directly reacted with 3-methoxy-5-oxocyclohex-3-ene-1-carboxylic acid **8** (i.e. 'protected dimedone residue', obtained following a literature procedure[13]) to yield compound **14**. However, this synthetic approach gave very low yields both for several of the reaction intermediates and for the final product **14** (*ca*. 6%). Therefore, we explored a different synthetic approach to obtain higher yields of **14**. We used Nα-Fmoc-Nε-Boc-L-Lys as protected scaffold to carry out the first reaction on the dipicolinic starting material **1** (Scheme 1). The coupling was performed with TBTU (2-(1*H*-benzotriazol-1-yl)-*N,N,N',N'*-tetramethylaminium tetrafluoroborate) and DIPEA in anhydrous DMF and resulted in a good conversion of **1** into intermediate **9** (93% yield). Fmoc was removed and **10** was coupled with the protected dimedone **8**[13] using HOBt, EDC and Et_3N, to give **11** in nearly quantitative yield. Removal of Boc afforded intermediate **12** which was then used to introduce the 7-methoxycoumarin fluorophore. Activation of the carboxylic group of **4** *via* the succinimidyl ester **13**[27] was carried out, allowing the synthesis of **14** in 98% yield. The significantly higher yields of **14**, and the easier purification and higher yields of the reaction intermediates, indicate that the second synthetic approach (going from **9** to **14**) is significantly more efficient than the first.

A basic/acidic one-pot hydrolysis was subsequently performed to convert **14** into the desired ligand **15** (Scheme 2), using sequentially LiOH and HCl to remove the methyl protections on picolinic esters and dimedone. Compound **15** was purified through preparative HPLC and used in the final complexation reaction with $VOSO_4$ to obtain the final dimedone-substituted optical probe **16** (Scheme 2) as a dark green solid.

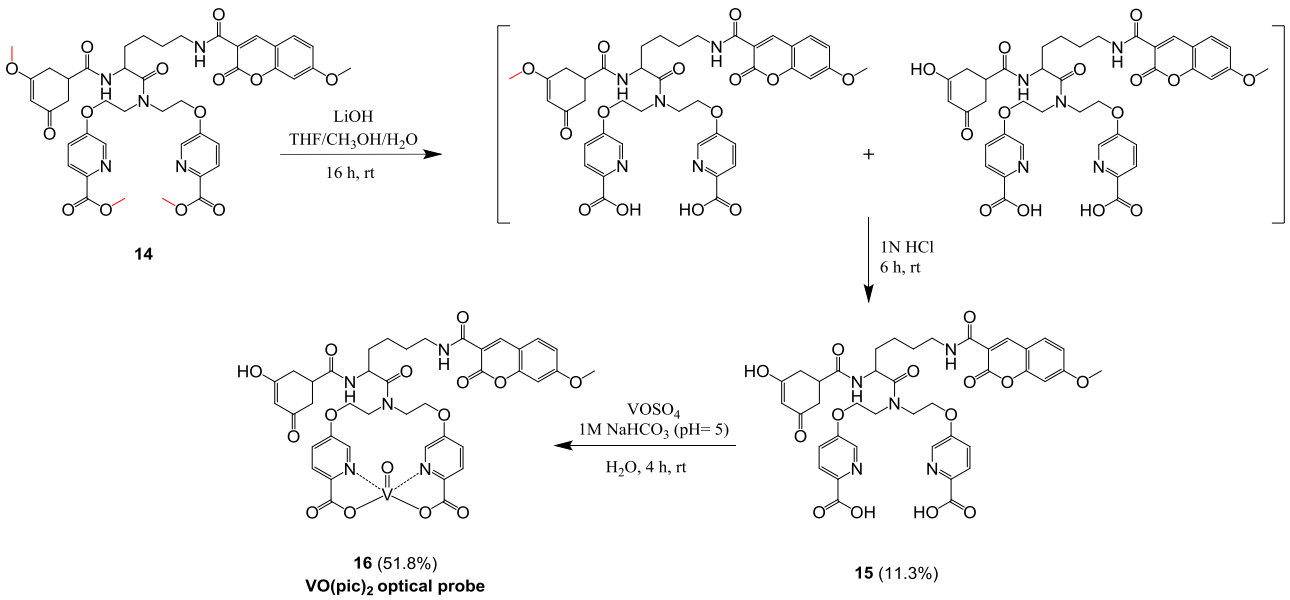

Scheme 2. Synthesis of the vanadyl complex **16**.

The formation of **16** was confirmed by mass spectrometry (ESI and MALDI - see Experimental section below and Section 4 in Supplementary Information for spectral data) which showed the molecular peak at 904 a.m.u. $[M+Na]^+$ and 880 a.m.u. $[M]^+$, respectively, and IR spectroscopy which showed the presence of a strong peak at 969 cm^{-1} (assigned to V=O). The presence of the vanadium(IV) centre was also confirmed by Electron Spin Resonance (ESR) studies in the solid state and solution (Figure 2 – see below for further discussion about ESR characterisation). Elemental analysis confirmed the formulation and purity of the complex. The vanadyl complex **16** also retained the optical properties of the coumarin moiety with an emission profile similar to the corresponding free ligand **15** (i.e. λ_{em} = 409 for ligand **15** and 407 nm for complex **16**; Sections 3 and 4 in Supporting Information).

To ensure that the L-Lys residue retained its configuration during standard coupling steps,[28] we performed enantio-resolution studies on **15** using three different chiral stationary phases (i.e. amylose tris(3,5-dimethylphenylcarbamate), cellulose tris(4-methylbenzoate), and cellulose tris(3,5-dimethylphenylcarbamate) in combination with two mobile phase systems (i.e. n-hexane/isopropanol

and acetonitrile/isopropanol).[29] These studies confirmed that racemization does not occur and the full synthetic route shows high stereoselectivity (Figure S1, Supporting Information).

Before carrying out cellular studies with complex **16**, it was of interest to establish its stability to oxidation under physiological conditions. To this end, we recorded the ESR spectra of **16** (at different times over 1 week) both as a solid and in solution using buffered aqueous media and 10% DMSO – which are the same solvents used to prepare the samples for the cellular studies described below. The sample of **16** used for these studies was prepared and stored under nitrogen prior to the ESR studies – which were carried out under aerobic conditions. As can be seen in Figure 2, the spectra at time zero and after 48 hours (both in the solid state and in solution) show clearly the presence of a vanadium(IV) species. However, after one week the ESR spectrum of the sample indicates that there is little vanadium(IV) left which is likely to be due to the oxidation of the metal centre to vanadium(V). This is not unusual for this type of complexes as has been previously reported by others.[30, 31]

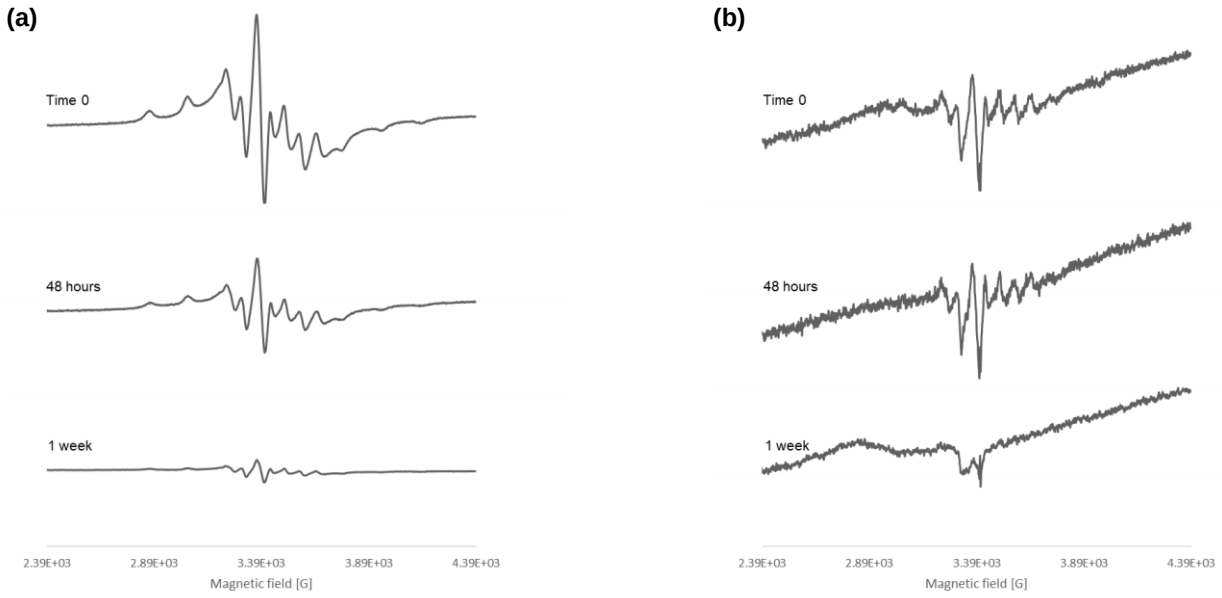

Figure 2. ESR spectra at 100 K for complex **16** (1 mg) suspended in McCoy's media (+10% DMSO, 200 μL). (a) Solid sample (4 scans) and (b) solution (16 scans) analysed at time 0 (i.e. the time when the complex was mixed with the solvent), 48 hours and after 1 week.

To assess further the possible oxidation of vanadium(IV) to vanadium(V), we recorded the ^{51}V NMR spectrum of a solution of complex **16** that had been exposed to air for 72 hours. This spectrum showed the presence of two very broad bands centred at *ca*. -490 and -700 ppm (see Figure S2). This NMR study indicates that vanadium(V) species formed over this period of time; however, the very broad peaks suggest that paramagnetic species (i.e. vanadium(IV)) are likely to be also present – which would be consistent with the ESR studies discussed above.

***In vitro* phosphatase inhibition studies.** As discussed above, VO-picolinate moieties have been previously shown to bind to a range of phosphatases (including CBPs) and inhibit their activity. Therefore, we were interested in establishing whether the new multi-functional probe **16** would still retain its ability to inhibit a selection of CBPs. For this, IC_{50} values were determined using 3-*O*-methylfluorescein phosphate (OMFP) as a substrate (see Experimental Section and Figure S4-6, Supporting Information).[32] These studies showed that **16** has a mid to high nanomolar inhibitory activity (IC_{50}= 99-221 nM, Table 1; Figure S5 and S6, Supporting Information) for a group of CBPs, including both tyrosine and lipid phosphatases (i.e. PTP1B, VHR, SHP-2, LMW-PTP and PTEN, see Table 1 for abbreviation). These observations are in agreement with our earlier investigation on the dansyl-labelled [$VO(pic)_2$] derivative (Figure 1(b)), which possessed similar potencies against PTPs and PTEN.[26] However, the IC_{50} values for **16** against VHR and PTP1B are around two-fold higher than for PTEN, SHP2 and LMW-PTP, whereas the dansyl-labelled [$VO(pic)_2$] derivative (see Figure 1(b)) favoured PTP1B, VHR and SHP2. This observation suggests that the new complex could have some selectivity towards specific CBPs compared to others, inhibiting better phosphatases with a

large catalytic pocket (e.g. PTEN),[33] or interacting with specific secondary substrate binding sites (e.g. in the case of SHP2 and LMW-PTP).[34]

Table 1. Inhibitory activity (IC_{50}, nM) of dimedone-based $VO(pic)_2$ complex **16** toward PTEN (= phosphatase and tensin homolog), VHR (= dual specificity protein phosphatase 3), SHP-2 (= Src homology region 2 domain-containing phosphatase-2), LMW-PTP (= low molecular weight protein tyrosine phosphatase), and PTP1B (= protein-tyrosine phosphatase 1B).

	PTEN	VHR	SHP2	LMW-PTP	PTP1B
16	99±13	199±15	113±2	106±4	221±12

Oxidation response in live cells. Having demonstrated the nanomolar affinity of **16** for a group of phosphatases, we next carried out flow cytometry and microscopy studies to determine whether the new probe would respond to changes in sulfenic oxidative modifications produced in cultured cells. Thus, probe **16** was first incubated (for 1, 6 and 24 hours) with live HCT116 cells, followed by flow cytometry to determine if **16** was cell permeable. However, the results showed that under these conditions the probe is unable to enter live cells (Figure S7, Supporting Information). Consequently, we next investigated cellular uptake in the presence of the phorbol ester PMA (i.e. phorbol 12-myristate-13-acetate), a fatty acid agent known to stimulate endocytosis.[35] We first determined cell viability using the MTS assay by incubating HCT116 cells with PMA (100 nM) and with **16** at different times (0 to 48 hours) and concentrations (0 to 200 μM). As can be seen in Figure S8, the viability of cells is not significantly compromised at incubations times of up to 7.5 h – even when the concentration of **16** was as high as 200 μM.

HCT116 cells were co-incubated for 1 and 6 hours with probe **16** (200 µM) and PMA (100 nM). In the presence of PMA, flow cytometry and microscopy analysis indicated an effective uptake of **16** in HCT116 cells at 6 hours (Figures S9 and S10, Supporting Information).

Having established a protocol to permeabilize live cells, we then carried out studies to assess the suitability of probe **16** to detect oxidative damage (see Experimental Section). Therefore, cells were co-treated with PMA (100 nM) and **16** (200 µM) for 6 h, followed by treatment with H_2O_2 (1 mM, 30 min) to generate protein SOHs. As can be seen in Figures 3 and S11 (Supporting Information) cells treated with H_2O_2 gave significantly higher fluorescence values with respect to controls (i.e. 0 mM **16** and 0 mM H_2O_2), suggesting that the optical probe is able to detect the oxidation produced upon addition of the oxidising agent.

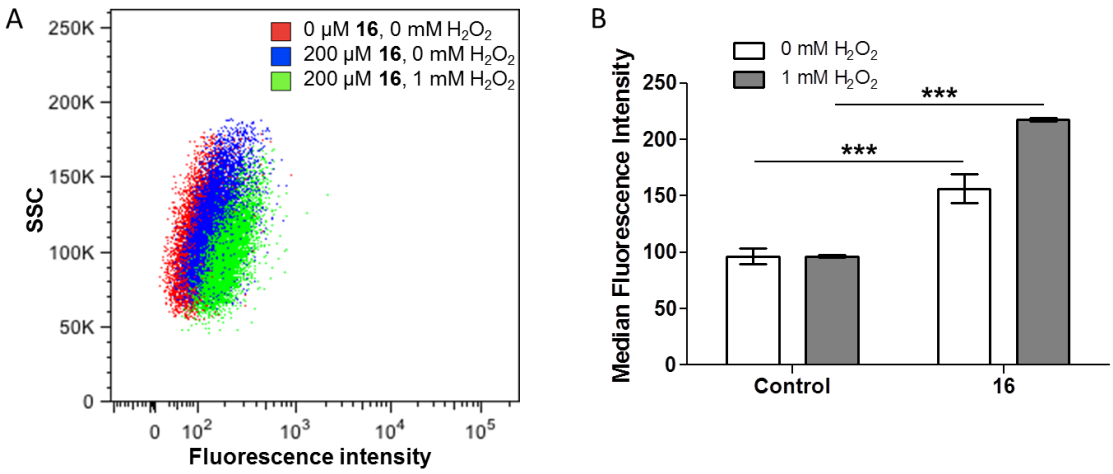

Figure 3. Flow cytometry analysis of HCT116 cells incubated with **16** under oxidative conditions. Live HCT116 cells were co-treated with 100 nM PMA and 200 µM **16** for 6 hours following by addition of 0 or 1 mM H_2O_2 for 30 min. A) Dotplot of **16** treated cells with (Green) and without (Blue) 1 mM H_2O_2 represent increase in fluorescence intensity upon treatment with H_2O_2. Untreated cells are shown in red. B) Increase of the median fluorescence intensity (MFI) observed in cells treated with 1 mM H_2O_2. Autofluorescence was measured in the absence of **16** (shown as control). MFI data are presented as mean ± SE of three independent experiments. 15000 cells were measured for each analysis. Significant differences (two-way ANOVA) to the control data are indicated by stars (***$p < 0.001$).

Employing the conditions used for flow cytometry it was also possible to image by fluorescence microscopy the oxidative formation of SOHs in HCT116 cells. Treatment was carried out on live cells which were then fixed and thoroughly washed to remove any unbound species (e.g. unreacted probe **16**). These experiments showed that there is some cellular uptake of **16** in live HCT116 cells (Figure 4(c), control 3) which is significantly increased upon treatment with H_2O_2 indicating successful crosslinking of the dimedone functionality in the cellular environment (Figure 4(d), oxidation experiment). As a control, we treated a sample of **16** (in buffer) with H_2O_2 for 30 minutes and compared its emission before and after treatment (see Figure S12). We observed an increase of the emission intensity after H_2O_2 treatment which could be due to a change in the oxidation state of the vanadium from V^{+4} (paramagnetic) to V^{+5} (diamagnetic). However, this on its own would not explain the great increase in emission observed in the H_2O_2-treated cells since, after treatment, cells were fixed and thoroughly washed to remove any unbound compound (either free **16** or unbound derivatives such as a vanadium(V) complex generated by oxidation with H_2O_2).

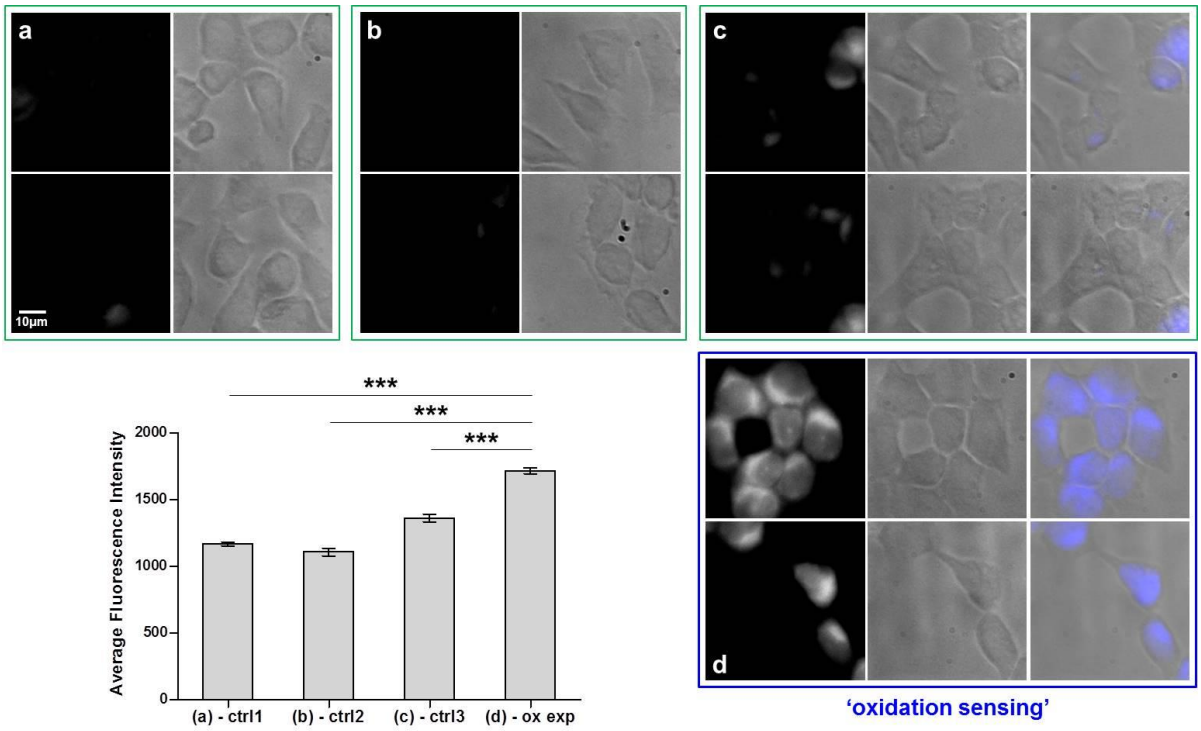

Figure 4. Fluorescence microscopy images showing uptake of **16** (blue) by live HCT116 cells and increase of fluoresce during ongoing oxidation (i.e. H_2O_2). (a) Control 1: no **16**, no H_2O_2. (b) Control 2: no **16**, 1 mM H_2O_2 for 30 min. (c) Control 3: 200 μM **16** (co-incubated with 100 nM PMA) for 6 hours, no H_2O_2. (d) 'Oxidation sensing' experiment: 200 μM **16** (co-incubated with 100 nM PMA) for 6 hours, 1 mM H_2O_2 for 30 min. Two representative images are presented for each treatment and comparison with merge channel images for **16** incubation experiments. Quantification of fluorescence signal was performed with FIJI. Data for the quantification are reported as mean ± SE and were obtained from a minimum of 3 independent experiments counting a total number of 12 cells for each treatment. Significant differences (5% cut-off for significance) to the control data are indicated by stars (***$p < 0.001$).

CONCLUSION

A multi-step synthetic protocol has been developed to prepare the new multifunctional probe **16**. This probe contains a validated CBP-targeting motif (i.e. the $VO(pic)_2$), a well-established SOH-reactive group (i.e. dimedone derivative) and an optical label (i.e. coumarine derivative) for *in vitro* and cellular imaging. To obtain this probe, a synthetic approach was performed where methyl-, Fmoc- and Boc- protecting groups were integrated into a tri-orthogonal protecting strategy, which proceeded with high enantioselectivity (i.e. L-Lys residue retains its chiral configuration). The reactions occur smoothly, leading to good yields of all the intermediates, and the overall mild conditions suggest that this procedure could be useful in complex molecule synthesis and related synthetic applications, relevant to picolinic acid functionalization in coordination chemistry research.[36] Our *in vitro* data indicates that **16** retains the nM affinity of the 'arrowhead' towards CBPs (analogous to recent results with the simpler $VO(pic)_2$ compound, shown in Figure 1(a)).[26] We have also demonstrated by preliminary flow cytometry and microscopy that the trifunctional probe can be taken up by live HCT116 cells (using a permeabilizing agent) and detect total changes in SOH levels upon treatment with H_2O_2. While our current data cannot confirm that CBPs are indeed being targeted inside the cell, it provides a first step towards the development of protein-selective intracellular probes to assess oxidative damage. Moreover, the established synthesis allows additional labelling methods (e.g. introduction of more emissive fluorophores) for further imaging approaches. However, it should be noted that while the vanadium(IV) centre in **16** does not oxidise significantly under aerobic conditions

within 48 hours, this is not the case under longer exposure times (between 3 and 7 days). Therefore, compound **16** might undergo redox changes once it is taken up by cells exposed to oxidative conditions (with H_2O_2). Future studies will aim to explore this in more detail.

EXPERIMENTAL DETAILS

General Considerations. All reagents were purchased from chemical suppliers and used without further purification, unless otherwise mentioned. Room temperature refers to ambient temperature. Yields refer to chromatographically and spectroscopically pure compounds unless otherwise stated. Where possible, reactions were monitored by thin layer chromatography (TLC) performed on commercially available glass plates pre-coated with Merck silica gel 60 F_{254} or Merck silica gel 60 RP-18 F_{254}s. Visualisation was by the quenching of UV fluorescence (λ_{max}= 254/365 nm) and by staining with iodine or potassium permanganate. All flash chromatography was carried out using slurry packed Merck 9325 Keiselgel 60 or Aldrich C_{18}-reverse phase silica gel. Solid-state infrared spectra were recorded neat on a Perkin–Elmer Spectrum 100 FT-IR spectrometer (operating region 4000 to 400 cm^{-1}) with internal referencing. Selected absorption maxima (λ_{max}) are reported in wavenumbers (cm^{-1}). Melting points were obtained using a Gallenkamp Melting Point apparatus and are uncorrected. Nomenclatures do not follow the IUPAC naming system. ^{1}H, ^{13}C, DEPT, HSQC, and COSY NMR spectra were recorded using an internal deuterium lock at ambient probe temperatures on a Bruker DRX-400 (400 MHz) instrument. Chemical shifts (δ) are quoted in ppm, to the nearest 0.01 ppm (for ^{1}H NMRs), or 0.1 ppm (for ^{13}C NMRs), and are referenced to the residual non-deuterated solvent peak. Coupling constants (J) are reported in Hertz (Hz) to the nearest 0.5 Hz. Data are reported as follows: chemical shift, multiplicity (br= broad; s= singlet; d= doublet; t= triplet; m= multiplet, or as a combination of these, e.g. dd, dt, etc.), integration, assignment and coupling

constant(s). Assignments were determined either on the basis of unambiguous chemical shift or coupling pattern, by patterns observed in 2D experiments (^{1}H-^{1}H COSY and HSQC, supported by DEPT) or by analogy to fully interpreted spectra for related compounds. Diastereotopic protons are assigned as CH-*H*. ^{51}V NMR spectra were recorded on a Bruker Avance 500 MHz instrument (scanning from 1400 to -2600 ppm) and using a sample prepared by dissolving 3 mg of the complex in *ca.* 400 μL of DMSO-d6. ^{51}V chemical shifts were referenced relative to neat sodium orthovanadate as the external standard. X-band ESR measurements were performed at 100 K using an X/Q-band Bruker Elexsys E580 Spectrometer (Bruker BioSpin GmbH, Germany) equipped with a closed-cycle cryostat (Cryogenic Ltd, UK) and a split-ring resonator with 2 mm sample access (ER 4118X-MS2). ESR samples were prepared by suspending 1 mg of the vanadium complex in 200 μL of McCoy's media (+10% DMSO p.a. grade) at room temperature. The sample was then loaded into 100mm Q Band Suprasil EPR Tubes (Wilmad-LabGlass) and flash-frozen in liquid nitrogen. Liquid chromatography–mass spectrometry (LC-MS) experiments were performed on Waters Aquity UPLC I-CLASS coupled with Waters LCT Premier (operating in ES^+ or ES^- mode), unless otherwise stated. High resolution masses (HR-MS) for accurate mass determination were performed on the same equipment and samples referenced against Leucine Enkaphalin or Sulfadimethoxine. For analytical HPLC, a Waters BEH Acquity C18 (50mm x 2.1mm) column was used and the mobile phase was composed of solvent A (99.9% Water, 0.1% Formic Acid) and solvent B (99.9% Acetonitrile, 0.1% Formic Acid) used in a linear gradient (time= 0 min, 95%A and 5%B; time= 3.2 min, 5%A and 95%B; time= 3.5 min, 95%A and 5%B; total run time 4 min). The sample solutions were prepared at a concentration of 0.1 mg/1 mL. The injection volume was 10μL, the flow rate was 0.5mL/min, the column temperature was 40 °C, and the UV detector wavelength was fixed at 210 to 280 nm. The values of retention time (t_R) are given in minutes. Unless otherwise mentioned, electron spray ionisation (ESI) conditions were as follow: 2kV (ES^+) and 2.5kV (ES^-) capillary voltage; 30 V (ES^+) and 150 V (ES^+) sample cone voltage; 2.1kV MCP Voltage; 350 °C desolvation temperature; 120 °C source temperature; 10 L/h cone gas flow (N_2); 400 L/h desolvation gas flow (N_2). Mass values are

reported within the error limits of ±5 ppm mass units. MALDI analyses were performed using MicroMass MALDI microMX TOF operating in reflectron mode using a 337nm nitrogen laser. Preparative HPLC purifications were performed using H_2O:CH_3OH (gradient from 95:5 to 5:95, over 18 min). The solvents were degassed and supplemented with 0.1% formic acid prior to use. HPLC platform consisted of a Waters RP-HPLC system (Waters 2767 autosampler for sample injection and collection; Waters 515 HPLC pump to deliver the mobile phase to the source; XBridge C_{18} columns with dimensions 19 mm x 100 mm) coupled to a Waters 3100 mass spectrometer (with ESI in positive and negative modes) and a Waters 2998 Photodiode Array (with detection between 200-600 nm). Microanalyses (C, H, and N) were performed by Mr. Alan Dickerson (University of Cambridge) and results are within ±0.4% of the theoretical values. Dimethyl-5,5'-{azanediylbis[(ethane-2,1-diyl)oxy]}dipicolinate **1**,[26] 3-methoxy-5-oxocyclohex-3-ene-1-carboxylic acid **8**[13] and *N*-succinimidyl ester of 7-methoxycoumarin-3-carboxylic acid **13**[27] were prepared by literature procedures.

***Boc/Fmoc-dipicolinate* (2).** HATU (1.35 g, 3.55 mmol) and DIPEA (1.85 mL, 10.64 mmol) were sequentially added to a solution of **1** (1.11g, 2.96 mmol) and *N*α-Boc-*N*ε-Fmoc-L-Lys (1.39 g, 2.96 mmol) in anhydrous DMF (20.0 mL) and the reaction was stirred for 7 h at 60 °C under N_2 atmosphere. The solvent was removed under reduced pressure and the mixture was directly purified by flash column chromatography (eluent: CH_2Cl_2/CH_3OH 95:5) to yield 450 mg (18.4% yield) of **2** as a yellowish viscous oil. ^{1}H NMR (400 MHz, $CDCl_3$) δ 8.35 (dd, 2H, ArH pic, *J*= 10.4 Hz, *J*= 2.8 Hz), 8.07 (t, 2H, ArH pic, *J*= 8.0 Hz), 7.75 (d, 2H, ArH Fmoc, *J*= 7.6 Hz), 7.57 (d, 2H, ArH Fmoc, *J*= 6.8 Hz), 7.38 (dd, 2H, ArH Fmoc, *J*= 6.8 Hz, *J*= 7.6 Hz), 7.29 (td, 2H, ArH Fmoc, *J*= 6.4 Hz, *J*= 1.2 Hz), 7.24-7.27 (m, 1H, ArH pic), 7.22 (dd, 1H, ArH pic, *J*= 5.6 Hz, *J*= 2.8 Hz), 5.20-5.25 (m, 1H, *CH*NH), 4.88 (exch br t, 1H, NH), 4.73-4.78 (m, 1H, *CH*CH_2O), 4.17-4.37 (m, 6H, 2 x CH_2CH_2O + $CHCH_2O$), 4.09-3.98 (m, 3H, NCH_2CH_2O + NCH-*H*CH_2O), 3.97 (s, 6H, OCH_3), 3.96 (s, 3H, OCH_3), 3.68-3.73 (m, 1H, NCH-*H*CH_2O), 3.10-3.18 (m, 2H, $(CH_2)_2CH_2N$), 1.41-1.67 (m, 15H, $CH(CH_2)_3$ + $(CH_3)_3$ Boc). LC-MS (ESI) calcd. for $C_{44}H_{51}N_5O_{11}$ 825.9 (MW), found *m/z* 826.4 $[M+H]^+$, t_R= 2.4.

***Amine dipicolinate* (3).** Intermediate **2** (450.0 mg, 0.54 mmol) was dissolved in CH_3CN (8.0 mL), piperidine (2.0 mL) was dropwise added and the reaction was stirred overnight at room temperature. After evaporation of the solvent under vacuum, the mixture was purified by flash column chromatography (eluent: CH_2Cl_2/CH_3OH 9:1) giving 170.0 mg (52.1% yield) of **3** as a pale yellow oil. ^{1}H NMR (400 MHz, $CDCl_3$) δ 8.32 (dd, 2H, ArH pic, *J*= 13.6 Hz, *J*= 2.8 Hz), 8.06 (t, 2H, ArH pic, *J*= 8.8 Hz), 7.30 (dd, 1H, ArH pic, *J*= 6.0 Hz, *J*= 2.8 Hz), 7.22 (dd, 1H, ArH pic, *J*= 5.6 Hz, *J*= 2.8 Hz), 6.13 (exch br t, 1H, NH), 5.27-5.33 (m, 1H, *CH*NH), 4.70-4.77 (exch br m, 2H, NH_2), 3.95-4.34 (m, 6H, 2 x CH_2CH_2O + NCH_2CH_2O), 3.94 (s, 3H, OCH3), 3.93 (s, 3H, OCH3), 3.66-3.71 (m, 1H, NCH-*H*CH_2O), 3.41-3.48 (m, 1H, NCH-*H*CH_2O), 3.07-3.29 (m, 2H, $(CH_2)_2CH_2N$), 1.30-1.70 (m, 15H, $CH(CH_2)_3$ + $(CH_3)_3$ Boc). LC-MS (ESI) calcd. for $C_{29}H_{41}N_5O_9$ 603.6 (MW), found *m/z* 604.3 $[M+H]^+$, 302.9 $[M+2H/2]^+$, t_R= 1.3.

***Boc-dipicolinate* (5).** HOBt (37.8 mg, 0.28 mmol), Et_3N (0.05 mL, 0.39 mmol) and EDC (0.07 mL, 0.39 mmol) were sequentially added to a stirred solution of 7-methoxycoumarin-3-carboxylic acid **4** (75.0 mg, 0.34 mmol) in anhydrous DMF (2.0 mL). Intermediate **3** (170.0 mg, 0.28 mmol) was added and the reaction was carried out for 48 h at room temperature under N_2 atmosphere. After removal of the solvent under vacuum, the crude mixture was purified by flash column chromatography (eluent: CH_2Cl_2/CH_3OH 95:5) to yield **5** (85.0 mg, 37.7% yield) as an oil. ^{1}H NMR (400 MHz, $CDCl_3$) δ 8.67 (dd, 1H, ArH coum, *J*= 2.8 Hz, J= 1.6 Hz), 8.34 (dd, 2H, ArH pic, *J*= 12.8 Hz, *J*= 2.8 Hz), 8.07-8.14 (m, 3H, ArH pic (2) + coum (1)), 7.94 (dd, 1H, ArH coum, *J*= 7.6 Hz, *J*= 1.2 Hz), 7.59 (dd, 1H, ArH coum, *J*= 4.4 Hz, *J*= 4.4 Hz), 7.33 (dt, 1H, ArH pic, *J*= 8.8 Hz, J= 2.8 Hz), 7.24 (dd, 1H, ArH pic, *J*= 6.0 Hz, *J*= 2.8 Hz), 6.01 (exch br s, 1H, NH), 5.22-5.34 (m, 1H, *CH*NH), 4.70-4.80 (exch br m, 1H, NH_2), 3.77-4.37 (m, 15H, 2 x CH_2CH_2O + NCH_2CH_2O + OCH_3 coum (overlapped, 4.12) + 2 x OCH_3 pic (overlapped, 3.97 and 3.96)), 3.66-3.74 (m, 1H, NCH-*H*CH_2O), 3.44-3.49 (m, 1H, NCH-*H*CH_2O), 3.10-3.30 (m, 2H, $(CH_2)_2CH_2N$), 1.32-1.68 (m, 15H, $CH(CH_2)_3$ + $(CH_3)_3$ Boc). LC-MS (ESI) calcd. for $C_{40}H_{47}N_5O_{13}$ 805.8 (MW), found *m/z* 806.3 $[M+H]^+$, 828.3 $[M+Na]^+$, t_R= 2.1.

***Fmoc/Boc-dipicolinate* (9). 1** (490.0 mg, 1.30 mmol), DIPEA (0.68 mL, 3.92 mmol) and TBTU (629.0 mg, 1.96 mmol) were sequentially added to a stirred solution of Nα-Fmoc-Nε-Boc Lys (609.0 mg, 1.30 mmol) in anhydrous DMF (10.0 mL) under N_2 atmosphere. The reaction was carried out for 6 h at room temperature. After removal of the solvent, the crude mixture was extracted with CH_2Cl_2 and a saturated solution of $NaHCO_3$. The organic layer was concentrated in *vacuo* and the residue was purified by flash column chromatography (eluent: CH_2Cl_2/CH_3OH 95:5) to obtain **9** as a yellowish oil (1.0 g, 93.1% yield). ^{1}H NMR (400 MHz, $CDCl_3$) δ 8.31 (dd, 2H, ArH pic, *J*= 19.2 Hz, *J*= 2.8 Hz), 8.01 (d, 2H, ArH pic, *J*= 8.8 Hz), 7.69 (dd, 2H, ArH Fmoc, *J*= 5.2 Hz, *J*= 2.8 Hz), 7.53 (d, 2H, ArH Fmoc, *J*= 7.2 Hz), 7.29-7.35 (m, 2H, ArH Fmoc), 7.19-7.25 (m, 3H, ArH Fmoc (2) + ArH pic (1)), 7.15 (dd, 1H, ArH pic, *J*= 6.0 Hz, *J*= 2.8 Hz), 5.71 (exch br d, 1H, NH), 4.74-4.80 (m, 1H, *CH*CH_2O), 4.58-4.65 (m, 1H, *CH*NH_2), 4.19-4.37 (m, 6H, 2 x CH_2*CH_2*O + CH*CH_2*O), 4.12 (t, 1H, NCH-*H*CH_2O, *J*= 7.2 Hz), 3.93-4.02 (m, 2H, N*CH_2*CH_2O), 3.92(s, 3H, OCH_3), 3.91(s, 3H, OCH_3), 3.65-3.73 (m, 1H, NCH-*H*CH_2O), 2.95-3.07 (m, 2H, $(CH_2)_2$*CH_2*N), 1.57-1.75 (m, 2H, CH*CH_2*$(CH_2)_2$), 1.24-1.51 (m, 13H, $CHCH_2$*$(CH_2)_2$* + $(CH_3)_3$ Boc). LC-MS (ESI) calcd. for $C_{44}H_{51}N_5O_{11}$ 825.9 (MW), found *m/z* 826.4 $[M+H]^+$, 848.4 $[M+Na]^+$, 413.9 $[M+2H/2]^+$, t_R= 2.4.

***Amine dipicolinate* (10).** A procedure analogous to the one used for the synthesis of **3**, using **9** (1.00 g, 1.21 mmol) as starting material and CH_3CN/piperidine 4:1 (12.0 mL), yielded pure **10** (730.0 mg, 99.9% yield) as a white solid (mp= 83-85°C), after purification by flash column chromatography (eluent: CH_2Cl_2/CH_3OH, gradient from 95:5 to 9:1). ^{1}H NMR (400 MHz, $CDCl_3$) δ 8.26 (dd, 2H, ArH, *J*= 15.2 Hz, *J*= 2.8 Hz), 7.95 (dd, 2H, ArH, *J*= 7.6 Hz, *J*= 0.8 Hz), 7.19 (dd, 1H, ArH, *J*= 6.0 Hz, *J*= 2.8 Hz), 7.95 (dd, 1H, ArH, *J*= 6.0 Hz, *J*= 2.8 Hz), 4.64-4.78 (m, 1H, *CH*NH_2), 4.24 (t, 2H, CH_2O, *J*= 5.2 Hz), 4.19 (t, 2H, CH_2O, *J*= 5.2 Hz), 3.76-4.00 (m, 9H, N*CH_2*CH_2O + NCH-*H*CH_2O + 2 x OCH_3 (overlapped, 3.86 and 3.85)), 3.64-3.72 (m, 1H, NCH-*H*CH_2O), 2.84-3.03 (m, 2H, $(CH_2)_2$*CH_2*N), 1.73-1.81 (m, 1H, CHCH-*H*$(CH_2)_2$), 1.52-1.65 (m, 1H, CHCH-*H*$(CH_2)_2$), 1.19-1.48 (m, 13H, $CHCH_2$*$(CH_2)_2$* + $(CH_3)_3$ Boc). LC-MS (ESI) calcd. for $C_{29}H_{41}N_5O_9$ 603.7 (MW), found *m/z* 604.3 $[M+H]^+$, 626.3 $[M+Na]^+$, 302.8 $[M+2H/2]^+$, t_R= 1.3.

***Boc-dipicolinate* (11).** HOBt (163.4 mg, 1.21 mmol), Et_3N (0.23 mL, 1.69 mmol) and EDC (0.30 mL, 1.69 mmol) were sequentially added to a stirred solution of 3-methoxy-5-oxocyclohex-3-ene-1-carboxylic acid **8** (288.0 mg, 1.69 mmol) in anhydrous DMF (10.0 mL) under N_2 atmosphere. A suspension of **10** (730.0 mg, 1.21 mmol) in anhydrous DMF (10.0 mL) was dropwise added and the reaction was carried out for 12 h at room temperature. After removal of the solvent under vacuum, the crude mixture was purified by flash column chromatography using CH_2Cl_2/CH_3OH 95:5 as eluent to obtain **11** (900.0 mg, 98.4% yield) as a yellowish solid (mp= 78-80°C). ^{1}H NMR (400 MHz, $CDCl_3$, signals marked with * correspond to additional peaks due to the presence of a minor isomer) δ 8.21 (dd, 2H, ArH, *J*= 16.0 Hz, J = 2.8 Hz), 7.93 (dd, 2H, ArH, *J*= 8.0 Hz, *J*= 1.6 Hz), 7.17-7.21 (m, 1H, ArH), 7.13 (dd, 1H, ArH, *J*= 5.6 Hz, *J*= 3.2 Hz), 5.17 (d*, 1H, *CH*$COCH_3$), 4.91-4.98 (m, 1H, *CH*NH), 4.74-4.85 (m*, 1H, *CH*NH), 4.21-4.31 (m, 2H, CH_2O), 4.08-4.17 (m, 2H, CH_2O), 3.84-4.00 (m, 3H, N*CH*$_2$$CH_2O$ + NCH-*H*CH_2O), 3.81(s, 3H, $COOCH_3$), 3.80 (s, 3H, $COOCH_3$), 3.56-3.64 (m, 1H, NCH-*H*CH_2O), 3.52 (d*, 3H, CHCO*CH*$_3$), 2.79-2.97 (m, 3H, NHCO*CH* + $(CH_2)_2$*CH*$_2$N), 2.61-2.69 (m, 1H, CHCH-*H*CO), 2.22-2.43 (m, 3H, CH*CH*$_2$CO + CHCH-*H*CO), 1.44-1.63 (m, 2H, CH*CH*$_2$$(CH_2)_2$), 1.14-1.37 (m, 13H, $CHCH_2$*(CH*$_2$*)*$_2$ + $(CH_3)_3$ Boc). LC-MS (ESI) calcd. for $C_{37}H_{49}N_5O_{12}$ 755.8 (MW), found *m/z* 756.4 $[M+H]^+$, 778.3 $[M+Na]^+$, 378.9 $[M+2H/2]^+$, t_R= 1.6.

***Amine dipicolinate* (12).** TFA (5.0 mL) was slowly added to a stirred solution of **11** (1.45 g, 1.92 mmol) in 10.0 mL of CH_2Cl_2 and the reaction was carried out for 2 h at room temperature. After removal of the solvent under vacuum, the crude mixture was purified by flash column chromatography (eluent: CH_2Cl_2/CH_3OH/NH_4OH 7:3:0.3) to give **12**·TFA (1.36 g, corresponding to 1.16 g of amine, 92.3% yield) as a brown viscous oil. ^{1}H NMR (400 MHz, CD_3OD, signals marked with * correspond to additional peaks due to the presence of a minor isomer) δ 8.33 (dt, 2H, ArH, *J*= 15.2 Hz, *J*= 2.8 Hz), 8.04 (dd, 2H, ArH, *J*= 8.8 Hz, *J*= 5.6 Hz), 7.52 (d, 1H, ArH, *J*= 8.0 Hz), 7.45 (dd, 1H, ArH, *J*= 6.0 Hz, *J*= 2.8 Hz), 5.37 (d*, 1H, *CH*$COCH_3$), 5.03-5.07 (m, 1H, *CH*NH (overlap CD_3OD, ppm values from $CDCl_3$ ^{1}H NMR)), 4.35-4.51 (m, 2H, CH_2O), 4.25-4.35 (m, 2H, CH_2O), 4.12-3.88 (m, 9H, N*CH*$_2$$CH_2O$ + NCH-*H*CH_2O + 2 x $COOCH_3$ (overlapped, 3.95 and 3.94)), 3.75-

3.86 (m, 1H, NCH-*H*CH_2O), 3.69 (d*, 3H, CHCO*CH_3*), 3.02-3.14 (m, 1H, NHCO*CH*), 2.81-2.94 (m, 2H, $(CH_2)_2$*CH_2*N), 2.38-2.72 (m, 4H, 2 x CH*CH_2*CO), 1.55-1.81 (m, 4H, CH*CH_2*CH_2*CH_2*), 1.31-1.52 (m, 2H, CHCH_2*CH_2*). LC-MS (ESI) calcd. for $C_{32}H_{41}N_5O_{10}$ 655.7 (MW), found *m/z* 656.3 $[M+H]^+$, 678.3 $[M+Na]^+$, 328.8 $[M+2H/2]^+$, t_R= 1.0.

***Dipicolinate* (14) -** *1st synthetic approach.* TFA (1.0 mL) was added to a stirred solution of intermediate **5** (85.0 mg, 0.10 mmol) in CH_2Cl_2 (2.0 mL). After 2 h at room temperature, the solvents were evaporated under vacuum to yield **6**·TFA as a brown oil (85.0 mg, crude sample), which was directly used in the next step without further purification. HOBt (13.5 mg, 0.10 mmol), Et_3N (0.02 mL, 0.14 mmol) and EDC (0.025 mL, 0.14 mmol) were sequentially added to a stirred solution of 3-methoxy-5-oxocyclohex-3-ene-1-carboxylic acid **8** (23.8 mg, 0.14 mmol) in anhydrous DMF (3.0 mL). Intermediate **6**·TFA (85.0 mg, 0.10 mmol) was added and the reaction was carried out for 48 h at room temperature under N_2 atmosphere. After removal of the solvent under vacuum, the crude mixture was initially purified by flash column chromatography (eluent: CH_2Cl_2/CH_3OH 95:5) and a following preparative HPLC purification was needed to obtain pure **14** (5.0 mg, yield 5.8% over 2 steps) as a thick yellow oil. ^{1}H NMR (400 MHz, $CDCl_3$, signals marked with * correspond to additional peaks due to the presence of a minor isomer) δ 8.71 (exch br t, 1H, NH), 8.67 (d, 1H, ArH coum, *J*= 6.4 Hz), 8.27 (dt, 2H, ArH pic, *J*= 19.6 Hz, *J*= 2.4 Hz), 8.00 (dd, 1H, ArH pic, *J*= 7.6 Hz, *J*= 1.2 Hz), 7.97 (d, 1H, ArH pic, *J*= 8.8 Hz), 7.50 (t, 1H, ArH coum, *J*= 8.8 Hz), 7.22-7.25 (m, 1H, ArH pic), 7.18 (dd, 1H, ArH pic, *J*= 6.0 Hz, *J*= 2.8 Hz), 6.81-6.85 (m, 1H, ArH coum), 6.73 (t, 1H, ArH coum, *J*= 2.4 Hz), 5.23 (d*, 1H, *CH*$COCH_3$), 4.90-4.99 (m, 1H, *CH*NH), 4.26-4.40 (m, 2H, CH_2O), 4.13-4.23 (m, 2H, CH_2O), 4.01-4.12 (m, 1H, NCH-*H*CH_2O), 3.91-4.02 (m, 2H, N*CH_2*CH_2O), 3.87 (s, 3H, $COOCH_3$), 3.85 (s, 3H, $COOCH_3$), 3.81 (d*, 3H, PhO*CH_3*), 3.59-3.70 (m, 1H, NCH-*H*CH_2O), 3.54 (d*, 3H, CHCO*CH_3*), 3.22-3.41 (m, 2H, $(CH_2)_2$*CH_2*N), 2.91-3.02 (m, 1H, NHCO*CH*), 2.65-2.72 (m, 1H, CHCH-*H*CO), 2.29-2.49 (m, 3H, CH*CH_2*CO + CHCH-*H*CO), 1.63-1.77 (m, 2H, CH*CH_2*$(CH_2)_3$), 1.44-1.61 (m, 2H, $CH(CH_2)_2$*CH_2*), 1.29-1.42 (m, 2H, $CHCH_2$*CH_2*). LC-MS (ESI)

calcd. for $C_{43}H_{47}N_5O_{14}$ 857.9 (MW), found *m/z* 858.3 $[M+H]^+$, 880.3 $[M+Na]^+$, 429.8 $[M+2H/2]^+$, t_R= 1.7. HR-MS (ESI) calcd. for $C_{43}H_{48}N_5O_{14}$ 858.3198 $[M+H]^+$, found *m/z* 858.3203.

Dipicolinate* (14)** - *2nd synthetic approach.** DMAP (14.5 mg, 0.12 mmol), **13** (358.9 mg, 1.13 mmol) and DIPEA (0.41 mL, 2.38 mmol) were sequentially added to a stirred solution of **12** (780.9 mg, 1.19 mmol) in anhydrous CH_2Cl_2 (5 mL) and the reaction was carried out under N_2 atmosphere for 10 h at room temperature. Additional DMAP (14.5 mg, 0.12 mmol), DIPEA (0.41 mL, 2.38 mmol) and **13** (50.0 mg, 0.16 mmol) were added and the mixture was stirred for further 12 h. After evaporation of the solvent under vacuum, the crude was directly purified by flash column chromatography using $CHCl_3$/CH_3OH 9:1 as eluent, affording **14** (1.00 g, 98.4% yield) as an oil. ^{1}H NMR, LC-MS and HR-MS match the characterization described above for **14** obtained through the "1st synthetic approach".

***Dipicolinic acid* (15) –** '*free' ligand.* LiOH (24.7 mg, 1.03 mmol) was added to a stirred solution of **14** (221.5 mg, 0.26 mmol) in THF (3.0 mL), CH_3OH (1.2 mL) and H_2O (1.2 mL). The reaction was stirred for 16 h at room temperature. After evaporation of the solvents, 1N HCl (3.0 mL) was added and the mixture was stirred for additional 6 h. 6N NaOH was slowly added until pH= 5 and solvents were then evaporated. The crude product was initially purified by reverse-phase column chromatography (eluent: CH_3OH/H_2O 1:1) and a following preparative HPLC purification was needed to obtain pure **15** (14.0 mg, yield 11.3% over 2 steps, one-pot) as a sticky yellowish solid. ^{1}H NMR (400 MHz, CD_3OD + D_2O, signals marked with * correspond to additional peaks due to the presence of a minor isomer) δ 9.00 (exch br s, 1H, NH), 8.74 (s, 1H, ArH coum), 8.29 (dd, 2H, ArH pic, *J*= 21.6 Hz, *J*= 2.8 Hz), 8.07 (dd, 2H, ArH pic, *J*= 8.8 Hz, *J*= 4.0 Hz), 7.69 (d, 1H, ArH coum, *J*= 8.8 Hz), 7.53 (dd, 1H, ArH pic, *J*= 6.0 Hz, *J*= 2.8 Hz), 7.48 (dd, 1H, ArH pic, *J*= 6.0 Hz, *J*= 2.8 Hz), 7.00 (dd, 1H, ArH coum, *J*= 6.4 Hz, *J*= 2.4 Hz), 6.94 (d, 1H, ArH, *J*= 2.4 Hz), 5.37 (s,* 1H, *CH*$COCH_3$ (*'enol form'*)), 4.97-5.04 (m, 1H, *CH*NH), 4.40-4.50 (m, 2H, CH_2O), 4.34 (t, 2H, CH_2O, *J*= 5.6 Hz), 4.02-4.13 (m, 3H, N*CH*$_2$$CH_2O$ + NCH-*H*CH_2O), 3.94 (s, 3H, PhO*CH*$_3$), 3.72-3.80 (m, 1H, NCH-*H*CH_2O), 3.40 (t, 2H, $(CH_2)_2$*CH*$_2$N, *J*= 5.6 Hz), 3.06-3.14 (m, 1H, NHCO*CH*), 2.66 (s,*

2H, $COCH_2CO$ (*'keto form'*)), 2.53-2.62 (m, 2H, $CHCH_2CO$), 2.40-2.48 (m, 2H, $CHCH_2CO$), 1.73-1.85 (m, 2H, $CHCH_2(CH_2)_3$), 1.57-1.67 (m, 2H, $CH(CH_2)_2CH_2$), 1.41-1.54 (m, 2H, $CHCH_2CH_2$). ^{13}C NMR (100 MHz, CD_3OD) δ 175.1 (2C), 175.0 (C), 168.1 (C), 166.8 (C), 166.7 (C), 164.5 (C), 163.3 (C), 158.9 (C), 158.7 (C), 157.8 (2C), 149.8 (CH), 142.1 (C), 141.9 (C), 138.3 (2CH), 132.6 (CH), 127.7 (2CH), 123.00 (CH), 122.8 (CH), 115.4 (CH), 114.9 (C), 113.4 (C), 111.2 (C), 101.2 (CH), 99.2 (CH*), 68.1 (CH_2), 67.5 (CH_2), 56.9 (CH_3), 50.87 (CH), 48.9 (CH_2), 48.3 (CH_2), 47.3 (CH_2), 41.0 (CH), 40.1 (CH_2*), 36.1 (CH_2), 35.6 (CH_2), 32.5 (CH_2), 29.6 (CH_2), 23.8 (CH_2). LC-MS (ESI) calcd. for $C_{40}H_{41}N_5O_{14}$ 815.8 (MW), found *m/z* 816.3 $[M+H]^+$, 838.3 $[M+Na]^+$, 408.8 $[M+2H/2]^+$, t_R= 1.3. UV-vis (H_2O): λ/nm 290, 353. Fluorescence (H_2O): λ_{max}(ex) 350 nm, λ_{max}(em) 407 nm; Φ_F = 0.11. HR-MS (ESI) calcd. for $C_{40}H_{42}N_5O_{14}$ 815.2728 $[M+H]^+$, found *m/z* 816.2727.

Chiral HPLC analyses of **15** were performed using Lux Amylose-1, Lux Cellulose-1, and Lux Cellulose-3 columns (150 x 2 mm, 3 µm I.D.; Phenomenex, Bologna, Italy) having amylose tris(3,5-dimethylphenylcarbamate), cellulose tris(3,5-dimethylphenylcarbamate), and cellulose tris(4-methylbenzoate) as chiral stationary phases respectively. All chromatographic resolutions were performed at 25°C using isocratic elution and mixtures of n-Hex/IPA or CH_3CN/IPA 90:10 as the polar modifier. The dead times (t_0) of the columns, estimated at flow rate of 1.0 mL/min, were comparable in the range of 0.9–1.0 min. From the analysis of the chromatogram obtained in analytical enantioseparations (Figure S1), we found that the chromatographic profiles of ligand **15** show only one main peak (> 95%) in all the three stationary phases tested, confirming that the *S* configuration of the L-Lysine is unchanged in the full synthetic pathway.

***VO(pic)$_2$ complex* (16)**. A solution of $VOSO_4 \cdot 3H_2O$ (15.2 mg, 0.07 mmol) in HPLC-grade H_2O (1.0 mL) was added dropwise to a stirred solution of **15** (57.0 mg, 0.07 mmol) in HPLC-grade H_2O (3.0 mL). 1M $NaHCO_3$ was added to adjust the pH to 5 and the reaction mixture was stirred for 4 h at room temperature. After 24 h, a precipitate formed which was recovered by filtration under vacuum to give **16** (40.0 mg, 51.8 % yield) as a dark green solid. MS (MALDI) calcd. for $C_{40}H_{39}N_5O_{15}V$

880.7 (MW), found *m/z* 880.5 $[M]^+$, 881.5 $[M+H]^+$. MS (ESI) calcd. for $C_{40}H_{39}N_5O_{15}V(HCOO)$, 925.7 (MW), found *m/z* 925.6 $[M]^+$, 947.6 $[M+Na]^+$, 963.6 $[M+K]^+$. IR: ν_{max} (neat)/cm^{-1} 3297 (OH), 2920 (NH), 1594 (CO), 969 (VO). UV-vis (DMSO): λ/nm 325. Fluorescence (DMSO): λ_{max}(ex) 350 nm, λ_{max}(em) 409 nm; Φ_F = 0.04. Anal. calcd. for $C_{40}H_{39}N_5O_{15}V(HCO_3)\cdot 9H_2O$: C, 44.6; H, 5.3; N, 6.3. Found: C, 44.2; H, 5.0; N, 6.4.

$VO(pic)_2$ complex **16** has been further analysed on a UPLC-MS/MS instrument consisting of a Waters ACQUITY liquid system equipped with a vacuum degasser, a binary pump, an autosampler and a thermostatted column compartment coupled to a Xevo TQ-S triple quadrupole mass spectrometer with an electron spray ionization source (ESI). The mass spectrometer was operated in positive ion mode and data were acquired using MassLynx V4.1 software. Analyses were conducted via direct injection in scan mode from 350 to 1000 m/z. Mass spectrometric conditions were as follows: capillary voltage 1.82 kV, source temperature 150 °C, desolvation temperature 150 °C, cone gas flow 150 L/h, desolvation gas flow 600 L/h, collision gas flow 0.11 L/h and nebulizer gas flow 7.00 bar, cone voltage 68.00 V. MS (ESI) calcd. for $C_{40}H_{39}N_5O_{15}V$, 880.7 (MW), found m/z 904.4 $[M+Na]^+$, 920.2 $[M+K]^+$.

UV-Vis and Emission Spectroscopy. *General Remarks.* The UV–vis spectra of the probes were recorded using a Perkin-Elmer Lambda 25 UV-vis spectrophotometer, while a Varian Cary Eclipse fluorescence spectrofluorimeter was used to record fluorescence emission spectra operating at a scan rate of 120 nm/min, using 0.05-0.1 mg/mL sample solutions and 1.0 cm path-length quartz cuvettes (1.0-3.0 mL) at 25°C. Spectra were not corrected for light intensity or detector sensitivity. Data were recorded on-line and analysed by Excel software on a PC computer.

Fluorescence quantum yield. For these measurements quinine sulphate was adopted as standard because it absorbs at the excitation wavelength appropriate to the samples, and emit in similar spectral regions. In order to minimize re-absorption effects, absorbances in the 10 mm fluorescence cuvette were kept below 0.1 at the excitation wavelength. Spectroscopic grade solvents were used and

checked for background fluorescence. The fluorescence of each sample was recorded in a range of 5 concentrations (absorbance values in the range 0.02–0.1) and plots of integrated fluorescence intensity (IF) *vs* absorbance (A) were recorded. The gradient of each plot (IF *vs* A) is proportional to the quantum yield of the sample (see Figure S3, Supporting Information). For each test sample, the Φ_F value was obtained relevant to the standard and represents the quantum yield value reported.

Biological studies on CBPs. *Expression and Purification.* PTP1B, VHR, SHP-2, PTEN and LMW-PTP were expressed as GST-fusion proteins. The protocol used was as follow. The corresponding RNA was extracted using PureLink® RNA Mini Kit from Invitrogen (according to manufacturer's protocol) from HEK293 cells. First DNA synthesis was performed using ProtoScript® First Strand cDNA Synthesis Kit from New England Biolabs according to manufacturer's protocol. In a second round of PCR, gene specific primers were used to obtain the DNA for PTEN, PTP1B, VHR, SHP2 and LMW-PTP, adding the restriction site BamHI at 5′ and XhoI at the 3′ end, respectively. The obtained coding regions of the respective DNA sequences were then cloned into pGEX-6P-1 vector using the aforementioned restriction sites. All four constructs were validated via DNA sequencing to ensure in-frame cloning with the GST tag encoded by the pGEX-6P-1 vector. Protein expression was induced in the E. coli strain DH5α for 24 h using 1 mM IPTG at 23° C. After growth the cells were harvested and stored at −20 °C. The harvested cells were resuspended in lysis buffer containing 50 mM Tris (pH 7.4), 1% Triton X-100, 10 mM benzamidine hydrochloride, 100 μg per mL soybean trypsin inhibitor, 1 mM 4-(2-aminoethyl)benzenesulfonyl fluoride hydrochloride and 2 mM DTT. Lysozyme was added to the cell suspension at a concentration of 2 mg/mL−1 and stirred for 1 h at 4 °C. Lysis was completed by sonication, followed by centrifugation at 18 000g for 30 min at 4 °C. The supernatant was loaded onto a glutathione sepharose column, pre-equilibrated with 50 mM Tris (pH 7.4), 140 mM NaCl and 2.7 mM KCl. After loading, the column was washed twice with 50 mM Tris (pH 7.4), 140 mM NaCl, 2.7 mM KCl and 2 mM DTT and 1% Triton X-100, another wash was performed using the same buffer without Triton X-100 and the final wash was carried out in the second buffer with 500 mM NaCl. The GST-tagged phosphatases were eluted using 20 mM

glutathione in 50 mM Tris (pH 7.4), 250 mM NaCl and 2 mM DTT. 50% glycerol was added and the proteins were stored at −80 °C. Protein concentration was determined using Bradford assay. Phosphatase activity was determined by OMFP assay (as an example, see Figure S4 Supporting Information).

Inhibition Assays (determination of IC_{50}). 3-O-methylfluorescein phosphate (OMFP, 10 mM in DMSO) was diluted with a 1% DMSO solution to 200μM. The vanadyl complex **16** was dissolved in DMF to 1 mM and further diluted in water containing 1% DMSO to the required concentrations. Assays were run in 100 mM Tris (pH7.4) containing 1 mM DTT at room temperature. The inhibitor solutions were incubated with the enzyme in the buffer for 10 minutes at room temperature before reaction was initiated by addition of OMFP. Hydrolysis of OMFP to OMF was monitored by measuring changes in fluorescence over 30 minutes at 60 s intervals (excitation 485 nm, emission 525 nm). Enzyme free blanks were run to eliminate background effects of OMFP hydrolysis in solution.

Cellular uptake and oxidative damage in live cells. HCT116 cells were co-incubated with 100 nM PMA and 200 μM **16** (DMSO was used as a vehicle control) for 1-6 hours. For oxidative damage experiment, 0 or 1 mM H_2O_2 was added 30 min before the end of incubation. After this, cells were washed three times with PBS and fixed (ice-cold 70% EtOH) or detached by trypsinisation, resuspended in PBS and analysed by microscopy or flow cytometry, respectively.

Flow cytometry and microscopy studies. *Cell culture and stock solutions.* HCT116 cells were cultured in McCoy's media (HyClone) in an atmosphere of 5% CO_2 at 37°C. All media was supplemented with 10% FBS (Invitrogen). **16** was dissolved in DMSO to a concentration 20 mM by 5 min sonication. For cell assays, a final 200 μM solution was prepared in cell mixture.

Cell viability: MTS assay. Cytotoxicity of complex **16** was measured by MTS assay (see Figure S8 for data). HCT116 cells were seeded in 96-well plate at three concentrations of $2.25x10^4$, $2x10^4$,

$1x10^4$ cells per well and were treated with mixture of [100 nM PMA + **16** at concentrations between 10 μM and 200 μM] for 7.5, 24 and 48 hours respectively. MTS/PMS reagents were added according to manufacture recommendations (Promega, G5421) and cell viability was calculated after measuring the absorption at 490 nm (as % of the control, i.e. cells treated with PMA but without added **16**). The results are shown as an average of triplicates ±SD using GraphPad Prism 7 software.

Uptake and oxidative damage experiments. *Flow cytometry.* Live cells were treated with 25 μg/ml propidium iodide (PI, Sigma). Subsequently, cells were filtered through 38 μm nylon filter mesh (Baldwin Filters Ltd, UK) and analysed on Fortessa flow cytometer using the laser excitation at 355 nm with 450/20 filter (for **16** uptake) and at 561 nm with 610/20 filter (for DNA profiles). From 10000 to 15000 events per sample were acquired. Cell aggregates and debris were excluded by gating on dot plots of side scatter pulse area (SSC-A) *vs* forward scatter pulse area (FSC-A) and forward scatter pulse area (FSC-A) *vs* forward scatter pulse width (FSC-W). Single cells were also gated on PI-Width and PI-Area plots. Profiles were analysed by plotting UV-fluorescence intensity using FlowJo software (Tree Star Inc, USA). Non-stained samples were used as a control of autofluorescence.

Microscopy. Fluorescence images were acquired using a Nikon Eclipse TE 2000-E inverted microscope and a PLAN FLUOR 40X air objective lens (NA = 0.60). A filter for UV2A (excitation wavelength 330-380 nm, long-pass emission wavelength 400 nm cut-on) was used and excitation light was provided by mercury lamp. Images of fixed cells were acquired using a Hammamatsu camera for each channel separately. Image analysis of mean fluorescence intensity was performed using Fiji-ImageJ.

Statistical analysis. Statistical comparison of the means (using GraphPad Prism 7) was performed by two-way ANOVA or two-tailed test (with a 5% cut-off for significance). The degree of significance is indicated by stars (i.e. *$p < 0.05$; **$p < 0.01$; ***$p < 0.001$) within the corresponding figures.

Acknowledgments. Authors gratefully acknowledge Mr M. Reynolds (ICL) for useful discussion on this research, Dr F. Mazzacuva (UCL) and Dr L. Haigh (ICL) for the help with MS analyses, Dr Enrico Salvadori (EPR facilities, QMUL), Mr Peter Haycock (NMR facilities, ICL), as well as Dr D. Mann (ICL) who kindly provided the HCT116 cells. This work was supported by the EPSRC-funded Proxomics Project (EP/I017887/1).

References

1) C. E. Paulsen and K. S. Carroll, *ACS Chem. Biol.*, 2010, **5**, 47–62.
2) C. E. Paulsen and K. S. Carroll, *Chem. Rev.*, 2013, **113**, 4633−4679.
3) K. E. Crump, D. G. Juneau, L. B. Poole, K. M. Haas and J. M. Grayson, *Eur. J. Immunol.*, 2012, **42**, 2152–2164.
4) G. Roos and J. Messens, *Free Rad.Biol. Med.*, 2011, **51**, 314–326.
5) R. L. M. van Montfort, M. Congreve, D. Tisi, R. Carr and H. Jhoti, *Nature*, 203, **423**, 773-777.
6) Y. Funato and H. Miki, *Methods*, 2014, **65**, 184-189.
7) M. Lo Conte and K. S. Carroll, *J. Biol. Chem.* 2013, **288**, 26480-26488.
8) N. J. Kettenhofen and M. J. Wood, *Chem. Res. Toxicol.*, 2010, **23**, 1633-1646.
9) L. B. Poole, P. A. Karplus and A. Claiborne, *Annu. Rev. Pharmacol. Toxicol.*, 2004, **44**, 325–347.
10) A. Claiborne, H. Miller, D. Parsinage and R. P. Ross, *FASEB J.*, 1993, **7**, 1483–1490.
11) H. S. Chung, S. B. Wang, V. Venkatraman, C. I. Murray and J. E. Van Eyk, *Circ.Res.*, 2013, **112**, 382-392.
12) J. Pan and K. S. Carroll, *Biopolymers*, 2014, **101**, 165-172.

13) K. G. Reddie, Y. H. Seo, W. B. Muse III, S. E. Leonard and Carroll, K. S. *Mol. BioSyst.*, 2008, **4**, 521–531.

14) R. L. Charles, E. Schröder, G. May, P. Free, P. R. J. Gaffney, R. Wait, S. Begum, R. J. Heads and P. Eaton, *Mol. Cell. Proteomics*, 2007, **6**, 1473-1484.

15) A. T. Saurin, H. Neubert, J. P. Brennan and P. Eaton, *Proc. Natl. Acad. Sci. U S A*, 2004, **101**, 17982–17987.

16) C. Klomsiri, K. J. Nelson, E. Bechtold, L. Soito, L. C. Johnson, W. T. Lowther, S. E. Ryu, S. B. King, C. M. Furdui and L. B. Poole, *Methods Enzymol.*, 2010, **473**, 77-94.

17) L. B. Poole, B.-B. Zeng, S. A. Knaggs, M. Yakubu and S. B. King, *Bioconjugate Chem.*, 2005, **16**, 1624-1628.

18) L. B. Poole, C. Klomsiri, S. A. Knaggs, C. M. Furdui, K. J. Nelson, M. J. Thomas, J. S. Fetrow, L. W. Daniel and S. B. King, *Bioconjugate Chem.*, 2007, **18**, 2004-2017.

19) T. F. Brewer, F. J. Garcia, S. Onak, K. S. Carroll and C. J. Chang, *Annu. Rev. Biochem.*, 2015, **84**, 765-790.

20) R. Karisch and B. G. Neel, *FEBS J.*, 2013, **280**, 459–475.

21) S. E. Leonard, F. J. Garcia, D. S. Goodsell and K. S. Carroll, *Angew. Chem. Int. Ed.*, 2011, **50**, 4423–4427.

22) F. J. Garcia and K. S. Carroll, *Eur. J. Med. Chem.*, 2014, **88**, 28-33.

23) C. C. McLauchlan, B. J. Peters, G. R. Willsky and D. C. Crans, *Coord. Chem. Rev.*, 2015, **301–302**, 163–199.

24) A. P. Seale, L. A. de Jesus, S. Y. Kim, Y. H. Choi, H. B. Lim, C. S. Hwang and Y. S. Kim, *Biotechnol. Lett.*, 2005, **27**, 221–225.

25) E. Rosivatz, J. G. Matthews, N. Q. McDonald, X. Mulet, K. K. Ho, N. Lossi, A. C. Schmid, M. Mirabelli, K. M. Pomeranz, C. Erneux, E. W. Lam, R. Vilar and R. Woscholski, *ACS Chem. Biol.*, 2006, **1**, 780–790.

26) J. Collins, A. Cilibrizzi, M. Fedorova, G. Whyte, L. H. Mak, I. Guterman, R. Leatherbarrow, R. Woscholski and R. Vilar, *Dalton Trans.*, 2016, **45**, 7104-7113.

27) G. R. Bardajee, M. A. Winnik and A. J. Lough. *Acta Cryst.*, 2007, **E63**, o1513–o1514.

28) A. Isidro-Llobet, T. Murillo, P. Bello, A. Cilibrizzi, J. T. Hodgkinson, W. R. J. D. Galloway, A. Bender, M. Welch and D. R. Spring, *Proc. Natl. Acad. Sci. U S A*, 2011, **108**, 6793-6798.

29) A. Cilibrizzi, L. Crocetti, M. P. Giovannoni, A. Graziano, C. Vergelli, G. Bartolucci, G. Soldani, M. T. Quinn, I. A. Schepetkin and C. Faggi, *Chirality*, 2013, **25**, 400–408.

30) T. Jakusch, W. Jin, L. Yang, T. Kiss and D. C. Crans, *J. Inorg. Biochem.*, 2003, **95**, 1-13.

31) T. Koleša-Dobravc, E. Lodyga-Chruscinska, M. Symonowicz, D. Sanna, A. Meden, F. Perdih and E. Garribba, *Inorg. Chem.*, 2014, **53**, 7960–7976.

32) L. H. Mak, R. Vilar and R. Woscholski, *J. Chem. Biol.*, 2010, **3**, 157-163.

33) S. J. Kim and S. E. Ryu, *BMB rep.*, 2012, **45**, 693-699.

34) L. M. Scott, H. R. Lawrence, S. M. Sebti, N. J. Lawrence and J. Wu, *Curr. Pharm. Des.*, 2010, **16**, 1843-1862.

35) A. Aballay, P. D. Stahl and L. S. Mayorga, *J. Cell Sci.*, 1999, **112**, 2549-2557.

36) P. Devi, S. M. Barry, K. M. Houlihan, M. J. Murphy, P. Turner, P. Jensen and P. J. Rutledge, *Sci. Rep.*, 2015, **5**, 9950; 10.1038/srep09950.